Supporting Information

Enargite (Cu_3AsS_4): A Ductile Mid-Temperature Thermoelectric Material

Prakash Govindaraj[a,b], Hern Kim[b,*], Kathirvel Venugopal[a,*]

[a]Department of physics and Nanotechnology, SRM Institute of Science and Technology, Kattankulathur, Chengalpattu, Tamil Nadu, India – 603 203

[b]Department of Energy Science and Technology, Environment Waste Recycle Institute, Myongji University, Yongin, Gyeonggi-do 17058, Republic of Korea

*Corresponding authors: hernkim@mju.ac.kr, kathirvv@srmist.edu.in

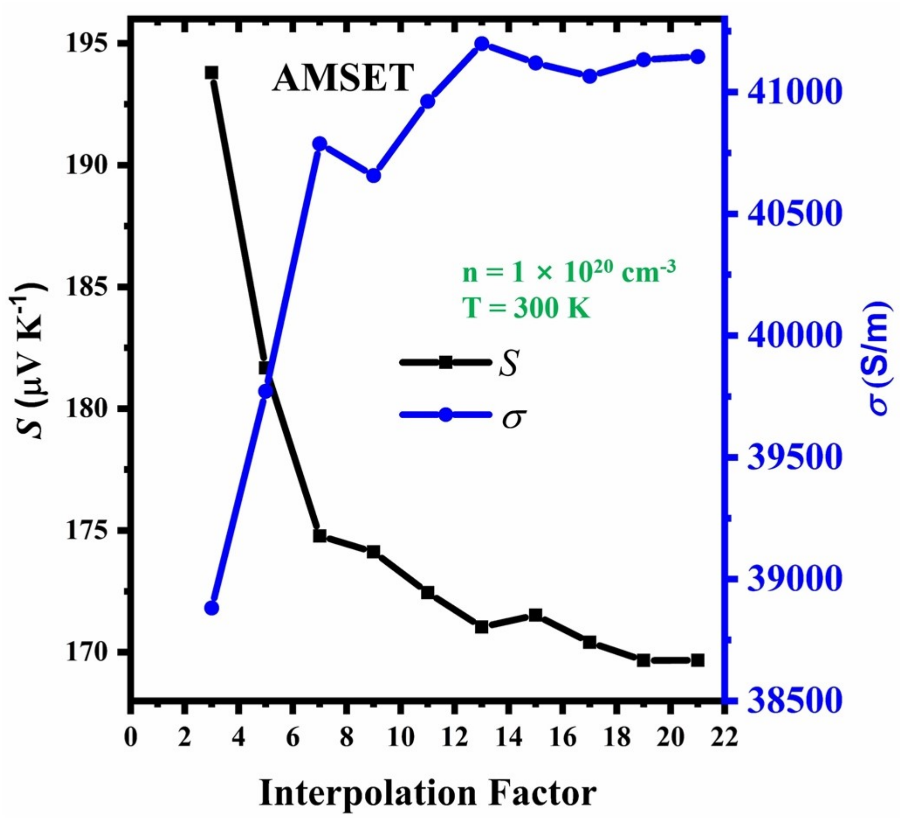

Fig. S1 AMSET - Interpolation factor convergence test at fixed temperature and carrier concentration.

S1.1. Cahill-Pohl and Slack model

Generally, the lattice thermal conductivity through Cahill and Slack model is manually estimated from elastic properties. The minimum lattice thermal conductivity is estimated by Cahill model[1] which is given by,

$$\kappa_{min} = \frac{k_B}{2.48} n^{2/3} (v_L + 2v_T) \tag{1}$$

The number density (n) is

$$n = \frac{Z}{V} \tag{2}$$

Where, Z - formula unit, V - volume of the unit cell (m^3).

The longitudinal and transverse sound velocity is given as[2]

$$v_L = \left(\frac{B + \frac{4G}{3}}{\rho} \right)^{\frac{1}{2}} \tag{3}$$

$$v_T = \left(\frac{G}{\rho} \right)^{\frac{1}{2}} \tag{4}$$

Where, B, G are estimated from Voigt-Reuss-Hill approximation.

The mass density (ρ, unit is g/cm^3) is

$$\rho = \frac{Z \times M.W}{N_A \times V} \tag{5}$$

Where, M.W – Molecular weight (g/mole), N_A – Avogadro number (6.022140×10^{23} $mole^{-1}$).

Further, the temperature dependent lattice thermal conductivity can be obtained from elastic constants through Slack model, expressed as,[3-5]

$$\kappa_L = A \frac{\bar{M}\,\theta_D^3 \delta}{\gamma^2 n^{2/3} T} \tag{6}$$

A – constant,

$$A = \frac{5.720 \times 10^7 \times 0.849}{2(1 - 0.514\gamma^{-1} + 0.228\gamma^{-2})} \tag{7}$$

The average atomic mass $\bar{M}$ is

$$\bar{M} = \frac{M.W}{n} \tag{8}$$

The Debye temperature θ_D is

$$\theta_D = \frac{h}{k_B} v_m \left(\frac{3N}{4\pi V}\right)^{1/3} \tag{9}$$

Here v_m is the average sound velocity, given by

$$v_m = \frac{1}{\left[\left[\frac{1}{3}\left(\frac{2}{v_T^3} + \frac{1}{v_L^3}\right)\right]\right]^{1/3}}$$

(10)

The average volume per atom δ is

$$\delta = \left(\frac{V}{n}\right)^{1/3} \tag{11}$$

N - number of atoms in the formula unit

$$Grüneisen\ parameter, \gamma = \frac{3}{2}\left(\frac{1 + v}{2 - 3v}\right) \tag{12}$$

$$Poisson's\ ratio, v = \frac{1 - 2\left(\frac{v_T}{v_L}\right)^2}{2 - 2\left(\frac{v_T}{v_L}\right)^2}$$

(13)

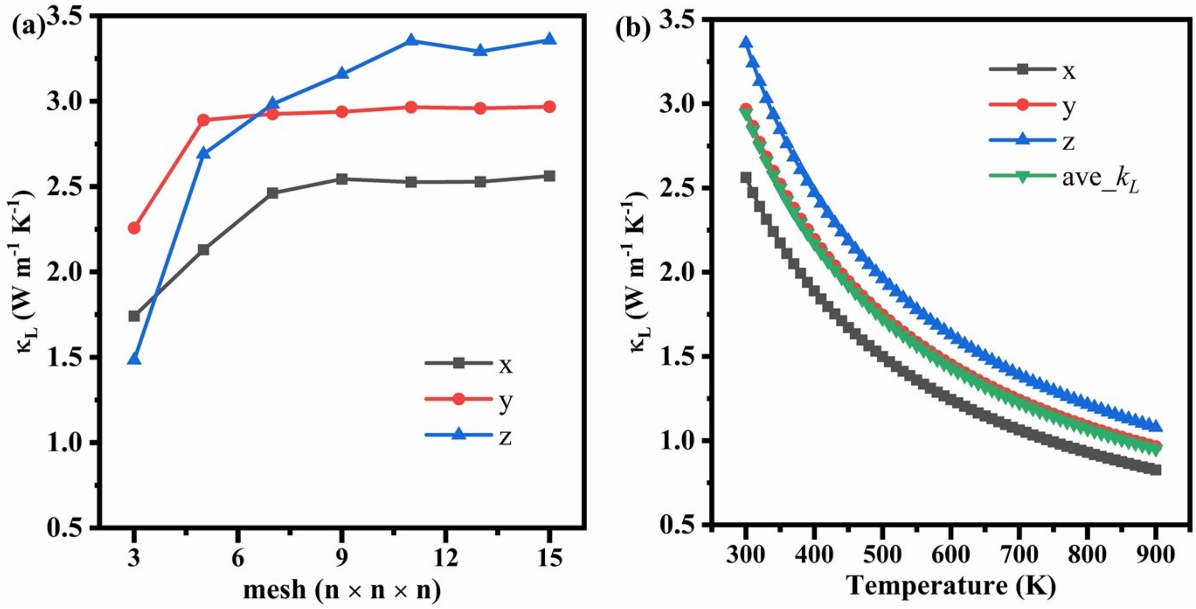

Fig. S2 (a) *q*-mesh Convergence test and **(b)** direction dependent lattice thermal conductivity against temperature for Cu_3AsS_4 using Phono3py with non-analytical term correction and isotopic scattering.

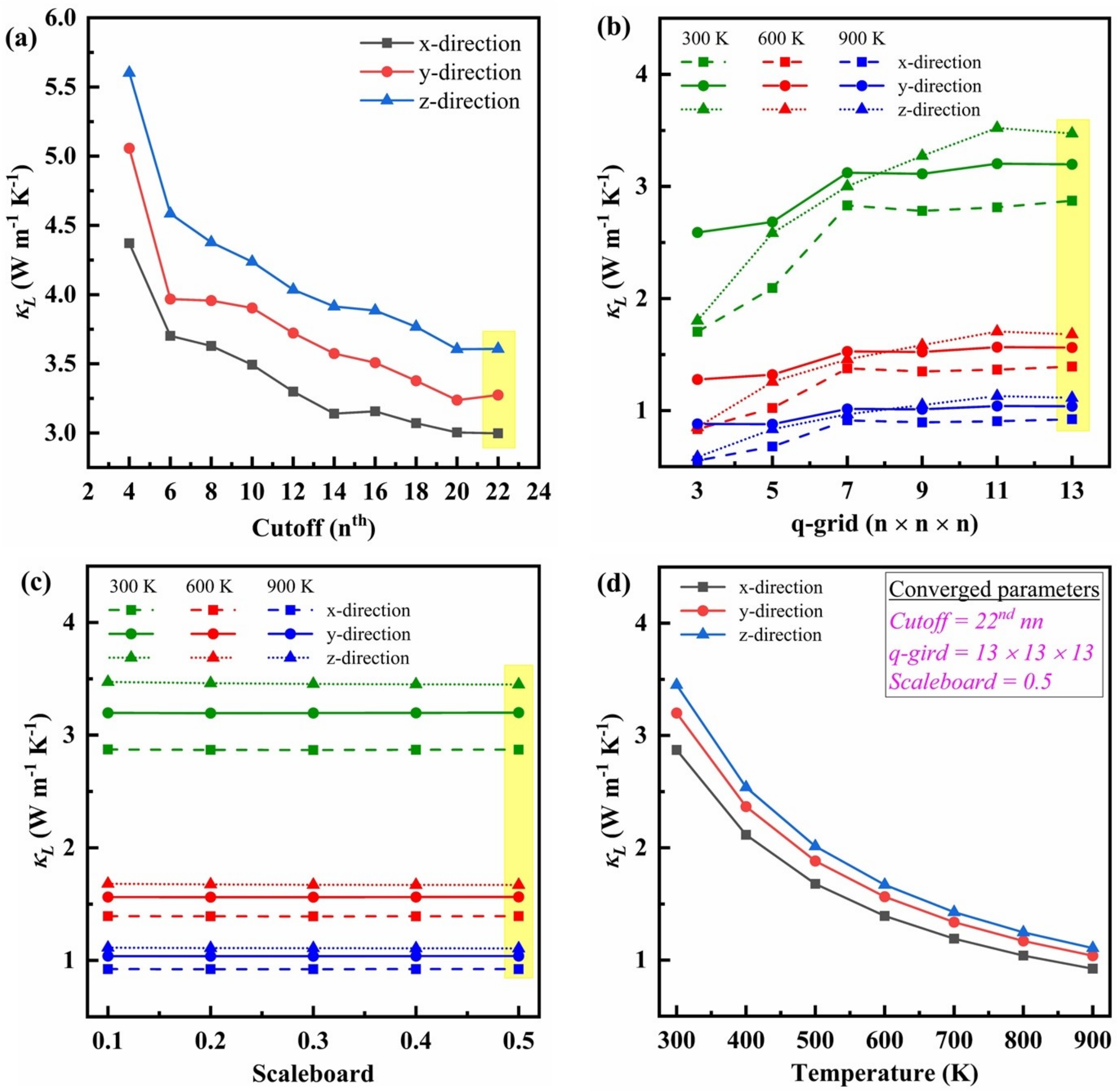

Fig. S3 (a) Cutoff distance, **(b)** q-grid and **(c)** scaleboard convergence test. **(d)** Direction dependent lattice thermal conductivity against temperature for Cu_3AsS_4 using ShengBTE.

S1.2. Transport properties of n-type Cu_3AsS_4

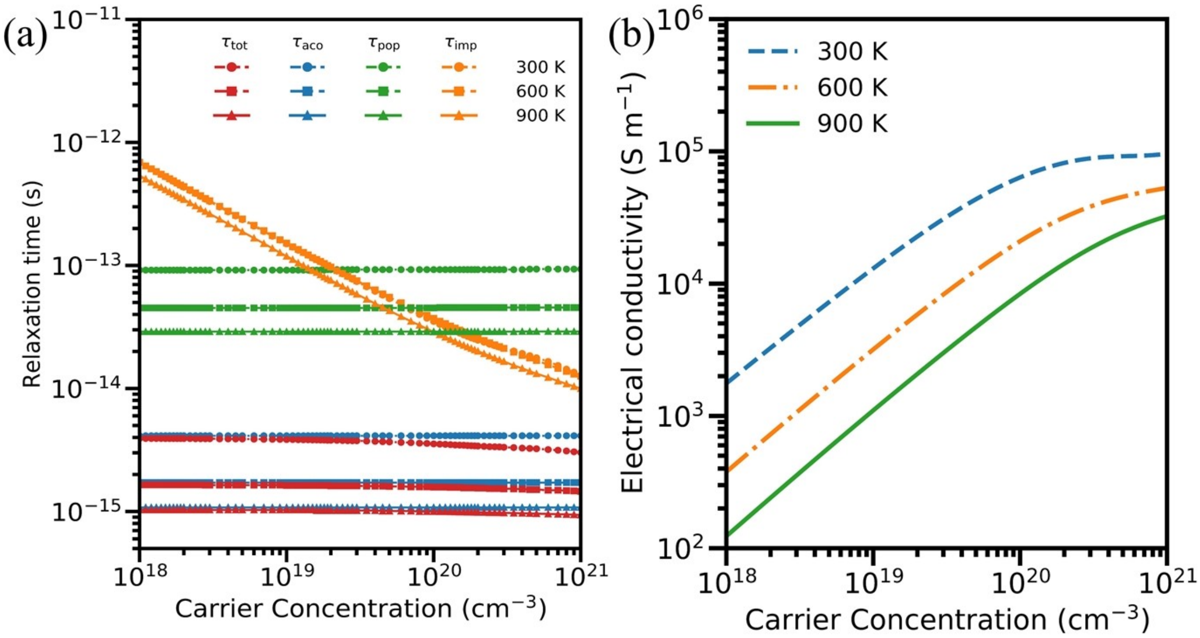

Fig. S4 (a) Relaxation time for electrons and **(b)** electrical conductivity for n-type Cu_3AsS_4

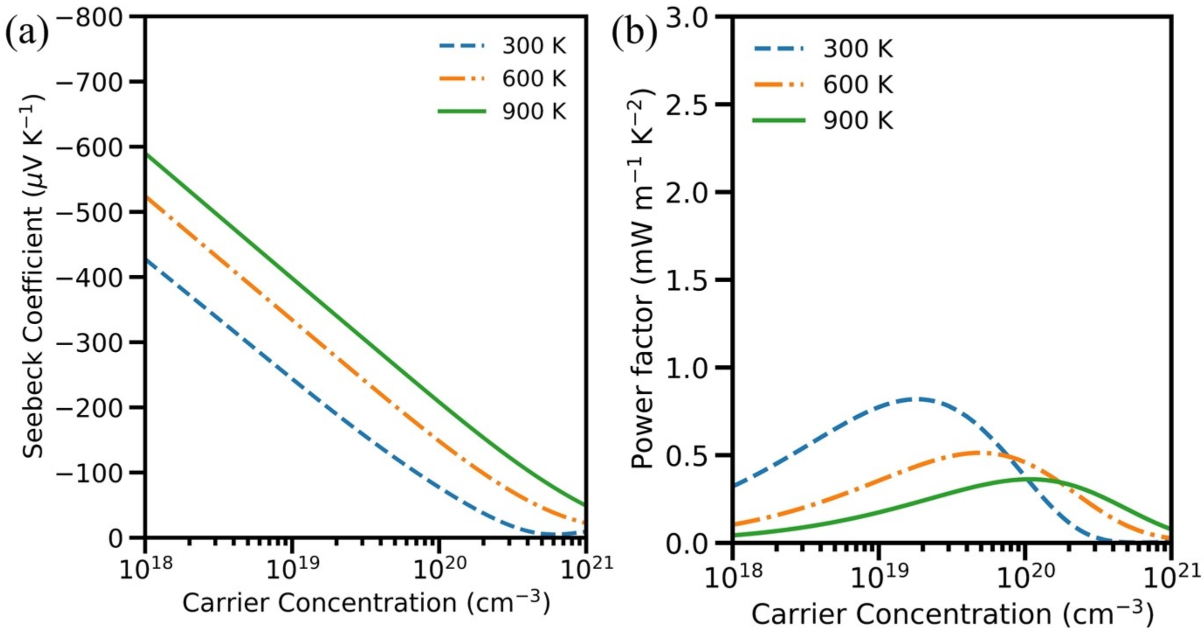

Fig. S5 (a) Seebeck coefficient and **(b)** power factor for n-type Cu_3AsS_4.

Table S1. Temperature dependent total relaxation time (τ_{tot}), electrical conductivity (σ) and Seebeck coefficient (S) for p- and n-type Cu_3AsS_4 for the carrier concentration of 1×10^{19} cm^{-3}.

Transport Properties	T **(K)**	**p-type Cu_3AsS_4**	**n-type Cu_3AsS_4**
τ_{tot} **(*fs*)**	300	11.9	3.85
	600	5.05	1.63
	900	2.98	1.03
σ **(S m^{-1})**	300	5019.89	13040.05
	600	2261.33	3183.02
	900	1397.83	1101.11
S ($\mu V\ K^{-1}$)	300	341	-243
	600	460	-334
	900	508	-398

Table S2. Comparison of the optimum thermoelectric power factor (PF) and corresponding carrier concentration (n) for p- and n-type Cu_3AsS_4 at 300 K, 600 K and 900 K.

Cu_3AsS_4	**T (K)**	**Optimum PF (mW m^{-1} K^{-2})**	***n*** **(cm^{-3})**
p-type	300	1.49	3.5×10^{20}
	600	1.90	4.0×10^{20}
	900	1.80	5.0×10^{20}
n-type	300	0.82	1.8×10^{19}
	600	0.51	5.0×10^{19}
	900	0.36	1.1×10^{20}

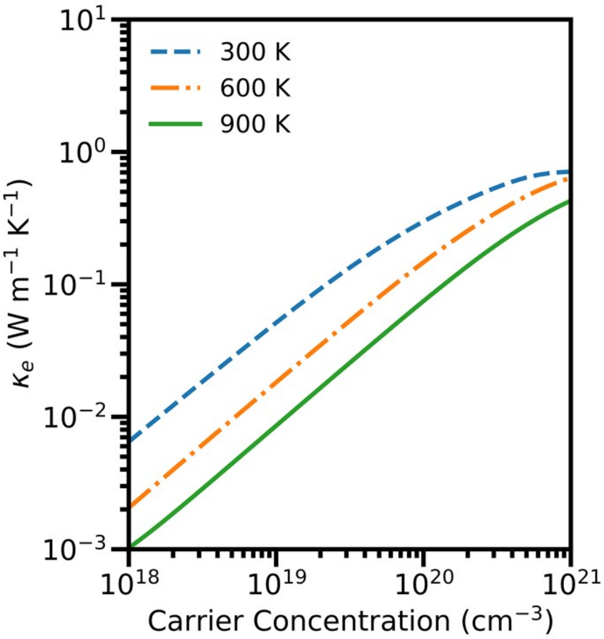

Fig. S6 Electronic thermal conductivity for n-type Cu_3AsS_4.

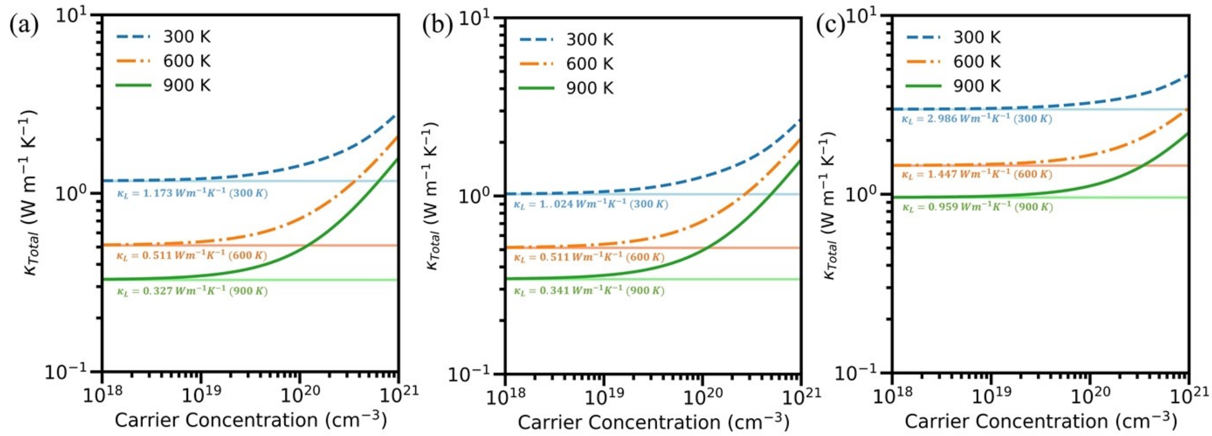

Fig. S7 Total thermal conductivity for p-type Cu_3AsS_4 with κ_L obtained from **(a)** mDC, **(b)** Slack and **(c)** PBTE-RTA approaches.

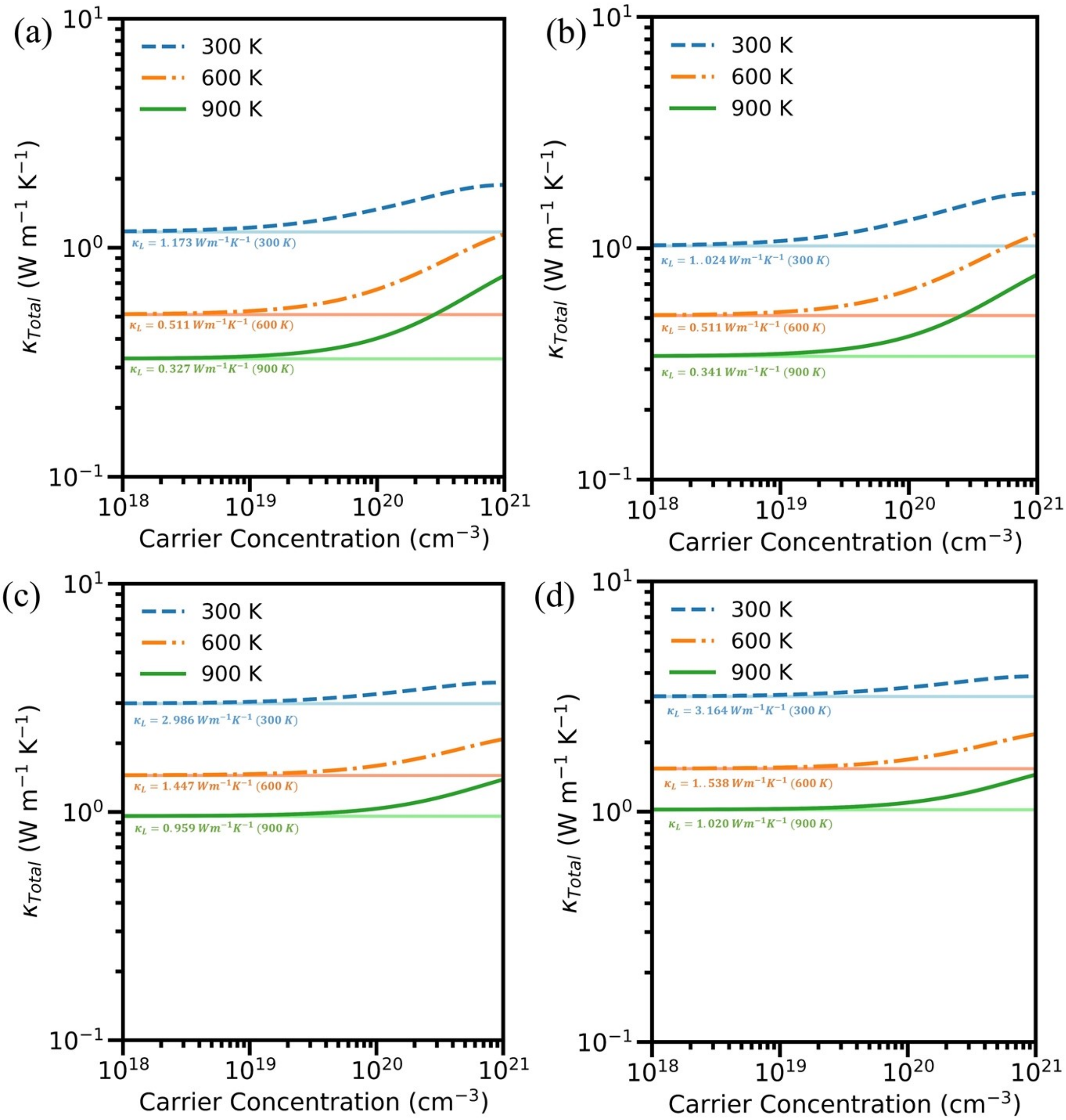

Fig. S8 Total thermal conductivity for n-type Cu_3AsS_4 with κ_L obtained from **(a)** mDC, **(b)** Slack, **(c)** PBTE-RTA, and **(d)** PBTE-Iterative approaches.

Table S3. Temperature dependent electronic thermal conductivity (κ_e) and total thermal conductivity (κ_{Total}) for p- and n-type Cu_3AsS_4. Four sets of κ_{Total} values are presented: each calculated with lattice thermal conductivity (κ_L) obtained from the mDC, Slack, PBTE-RTA and PBTE-Iterative approaches. For better comparison, all the values are given for the carrier concentration of 1×10^{19} cm^{-3}.

Transport Properties	T **(K)**	**p-type Cu_3AsS_4**	**n-type Cu_3AsS_4**
κ_e **($W\ m^{-1}\ K^{-1}$)**	300	0.034	0.051
	600	0.024	0.018
	900	0.017	0.008
κ_{Total} **($W\ m^{-1}\ K^{-1}$) (κ_L from mDC)**	300	1.207	1.224
	600	0.535	0.529
	900	0.344	0.336
κ_{Total} **($W\ m^{-1}\ K^{-1}$) (κ_L from Slack)**	300	1.058	1.075
	600	0.536	0.530
	900	0.358	0.349
κ_{Total} **($W\ m^{-1}\ K^{-1}$) (κ_L from PBTE-RTA)**	300	3.020	3.037
	600	1.471	1.465
	900	0.976	0.967
κ_{Total} **($W\ m^{-1}\ K^{-1}$) (κ_L from PBTE-Iterative)**	300	3.199	3.216
	600	1.562	1.556
	900	1.038	1.029

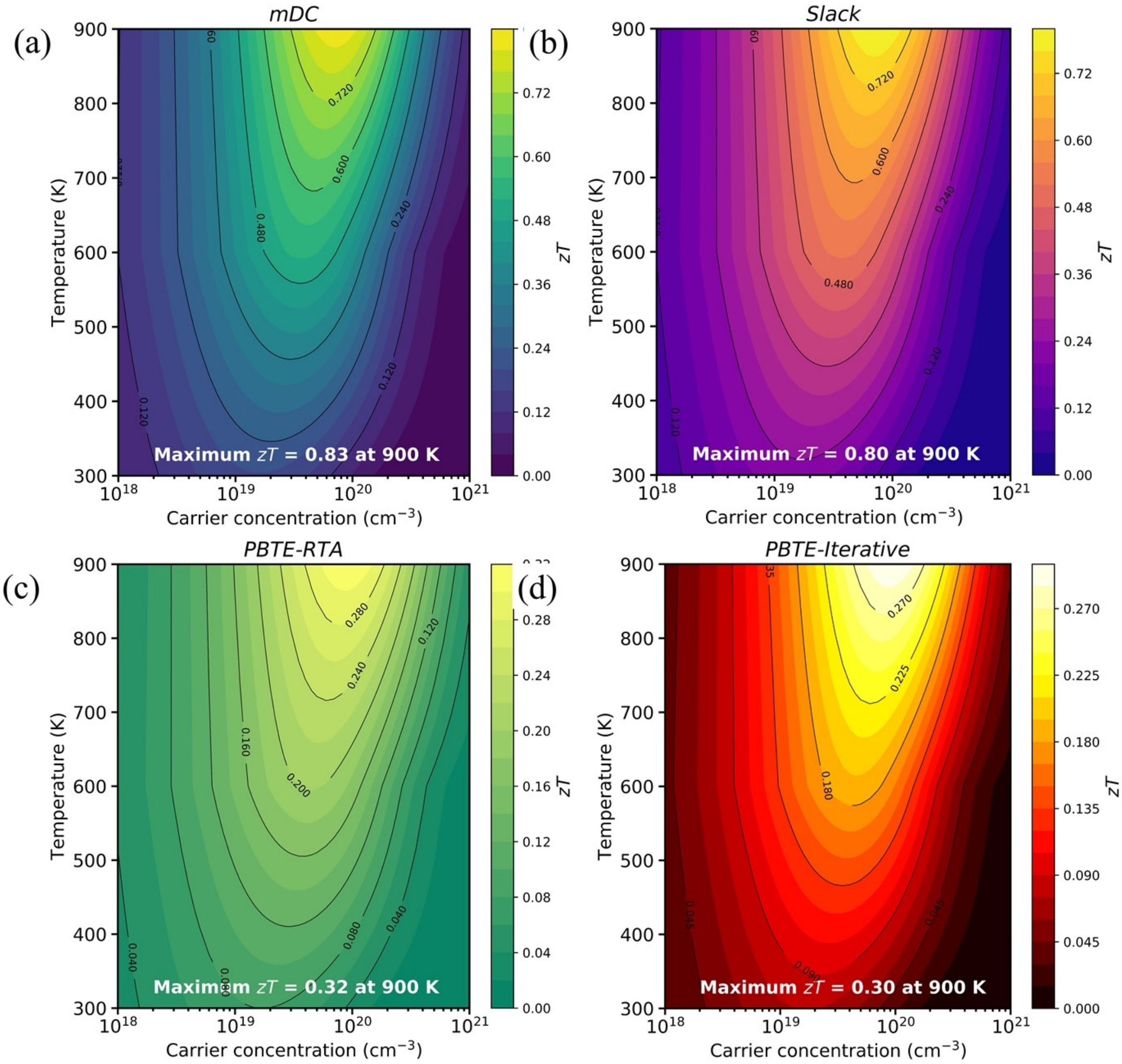

Fig. S9 The calculated zT for n-type Cu_3AsS_4 with κ_L derived from **(a)** mDC, **(b)** Slack, **(c)** PBTE-RTA, and **(d)** PBTE-Iterative approaches.

Table S4. Optimum Figure of merit (*zT*) and corresponding carrier concentration (*n*) for p and n-type Cu_3AsS_4 at different temperatures (300 K, 600 K and 900 K), computed using four different phonon transport approaches such as mDC, Slack, PBTE-RTA and PBTE-Iterative.

Approaches used to calculate k_L	**T (K)**	**p-type**		**n-type**	
		zT	***n*** **(cm^{-3})**	*zT*	***n*** **(cm^{-3})**
mDC	300	0.26	1.9×10^{20}	0.20	1.6×10^{19}
	600	1.19	1.3×10^{20}	0.53	4.0×10^{19}
	900	2.31	1.4×10^{20}	0.83	7.0×10^{19}
Slack	300	0.29	1.8×10^{20}	0.22	1.5×10^{19}
	600	1.19	1.3×10^{20}	0.53	4.0×10^{19}
	900	2.25	1.4×10^{20}	0.80	7.0×10^{19}
PBTE-RTA	300	0.12	2.6×10^{19}	0.08	1.6×10^{19}
	600	0.57	2.2×10^{19}	0.20	4.0×10^{19}
	900	1.12	2.4×10^{19}	0.32	9.0×10^{19}
PBTE-Iterative	300	0.12	2.6×10^{19}	0.06	4.0×10^{19}
	600	0.54	2.2×10^{20}	0.19	4.5×10^{19}
	900	1.07	2.4×10^{20}	0.30	9.0×10^{19}

References

1. D. G. Cahill, A. Melville, D. G. Schlom and M. A. Zurbuchen, *Applied Physics Letters*, 2010, **96**.

2. W. Chen, J.-H. Pöhls, G. Hautier, D. Broberg, S. Bajaj, U. Aydemir, Z. M. Gibbs, H. Zhu, M. Asta and G. J. Snyder, *Journal of Materials Chemistry C*, 2016, **4**, 4414-4426.

3. C. Loftis, K. Yuan, Y. Zhao, M. Hu and J. Hu, *The Journal of Physical Chemistry A*, 2020, **125**, 435-450.

4. D. T. Morelli, G. A. Slack, S. L. Shindé and J. S. Goela, in *High Lattice Thermal Conductivity Solids*, Springer, 2006.

5. G. A. Slack, R. A. Tanzilli, R. Pohl and J. Vandersande, *Journal of Physics and Chemistry of Solids*, 1987, **48**, 641-647.